

1 Supplementary Material

1.1 Videos

All the videos are taken from a portion of the real system size to show the system behaviour perceptibly.

Movie_Passive_Pes20.mp4: The movie of the simulation with passive colloids at $Pe_s = 20$. The snapshots in Fig. 3 of the main paper are taken from this movie. The system starts from the hexagonal crystal phase and the subsequent shearing promotes the sliding layers throughout the melting. The local ordered regions emergent due to the zig-zag motion of particles in these sliding layers are distinguishable at times.

Movie_Pea20_interstitialdefects.mp4: The movie for the simulation with active colloids ($Pe_a = 20$) under shearing ($Pe_s = 20$), shows that the self-propulsion assists the shear in disordering the system by promoting the interstitial defects. Every particle i is colored with respect to its local hexagonal order parameter, $\psi_{6,i}$, to show the extent of disordered/ordered regions in the domain.

Movie_shear thinning.mp4: The movie corresponds to the shear-thinning regime, i.e. $Pe_a = 30$. The colloidal suspension here is melted entirely by self-propulsion. After imposing the shear, the particles start to reorganise and cause a layered flow, which is a peculiar behaviour of shear-thinning fluids. Some locally ordered domains appear at times due to the zig-zag motion of particles under shear flow.

Movie_Newtonain.mp4: The movie corresponds to the Newtonian regime, i.e. $Pe_a = 70$. Colloids are homogeneously disordered by self-propulsion.

Movie_shear thickening.mp4: The movie corresponds to the shear-thickening regime, i.e. $Pe_a = 150$, the so-called the motility-induced shear thickening (MIST). Self-propulsion induces structural heterogeneity and clustering in the system.

1.2 The accumulation of disordered regions with activity

We located the position of defects by an analysis of the Voronoi cells. Voronoi cells with five or seven neighbour edges are indicative of defect positions. In the passive suspension, the defects appear due to the disordering effect of the shear (see Fig.1(a)). However, at the same time, defects can disappear while another one appears in another region. For the active suspensions, there are two forces in the system for the hexagonal-to-liquid transition: (i) shear and (ii) self-propulsion. The presence of the self-propulsion inhibits the disappearance of the defects, creating also some additional defects at the same time. Therefore, the defects can accumulate and spread over the domain as the activity increases. This scenario is confirmed by Fig.1(b), where the Voronoi diagram for $Pe_a = 20$ is illustrated.

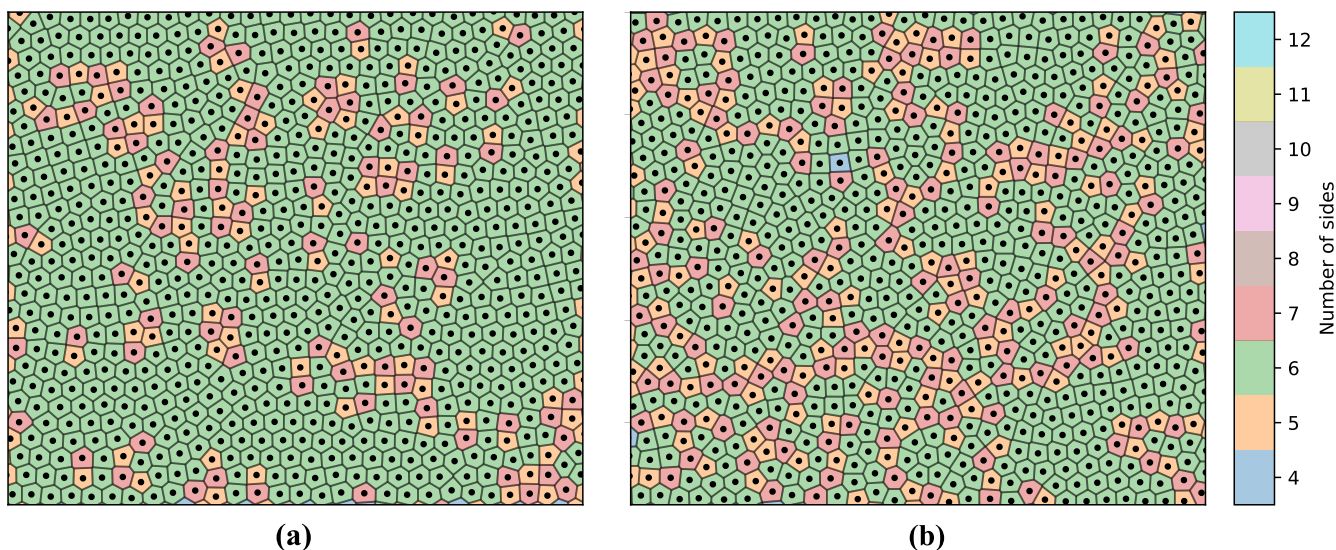


Fig. 1 The Voronoi diagrams for the colloidal suspension at the same shear rate ($Pe_s = 20$) for (a) $Pe_a = 0$ (i.e, the passive case) and (b) $Pe_a = 20$. These diagrams illustrate the accumulation of disordered regions (symptoms of the presence of defects) with increasing activity, resulting in an enhanced melting of the colloidal suspension

1.3 Solid-like regime for the passive and weakly active suspensions

We reproduce Fig. 3(a) of the manuscript by indicating the corresponding time averaged hexagonal order parameter $\overline{\psi}_6$ of the colloidal suspension at different shear rates and self-propulsions. Looking at $\overline{\psi}_6$ values here in Fig.2, we see that the passive suspension and the low activity case (i.e., $Pe_a = 10$) cannot reach a fully liquid regime ($\overline{\psi}_6 = 0$) over the shear range worked in this study. For these two cases, some ordered regions are still present in the suspension at different shear rates. The degree of order depends on the dominant mechanism (either shear ordering or disordering) at the corresponding shear rate. Starting with $Pe_a > 0$, activity helps the shear in disordering the system, but it still cannot melt the suspension homogeneously until reaching $Pe_a \geq 40$. Therefore, we obtain a different rheological response for these two cases compared to the active suspensions with $Pe_a \geq 40$. On the other hand, the active suspensions ($Pe_a \geq 40$) homogeneously show liquid behaviour ($\overline{\psi}_6 = 0$) with a rheological response that can be modelled by using the Herschel Buckley constitutive relationship.

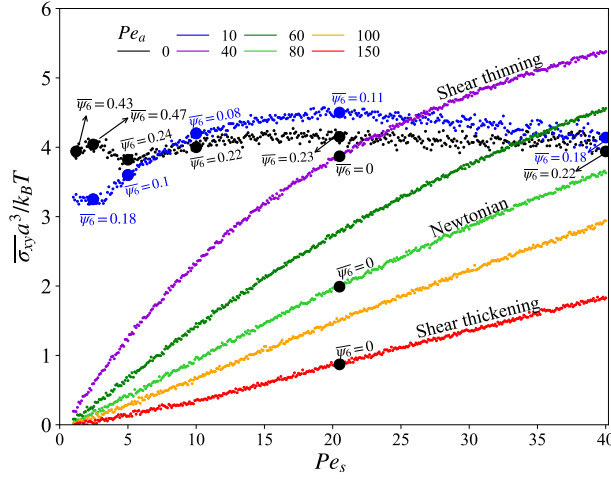


Fig. 2 The nondimensional shear stress $\overline{\sigma}_{xy}$ - shear rate $\dot{\gamma}$ curves for the passive ($Pe_a = 0$) and self-propelled ($Pe_a > 0$) systems. Note that the shear rates are shown starting with $Pe_s \geq 1$. This figure is equivalent to Fig. 3a of the main manuscript but with adding the value of $\overline{\psi}_6$ found for different values of the shear rates.

1.4 Apparent viscosity in the fully liquid regime

Since we obtained the shear thinning-to-thickening transition in the liquid-like regime, we show here the viscosity as a function of Pe_s for $Pe_a \geq 40$. As already illustrated by Fig.3(b) of the manuscript, Fig.3 confirms that a change in the regime between shear thinning and shear thickening occurs around $Pe_a = 90$.

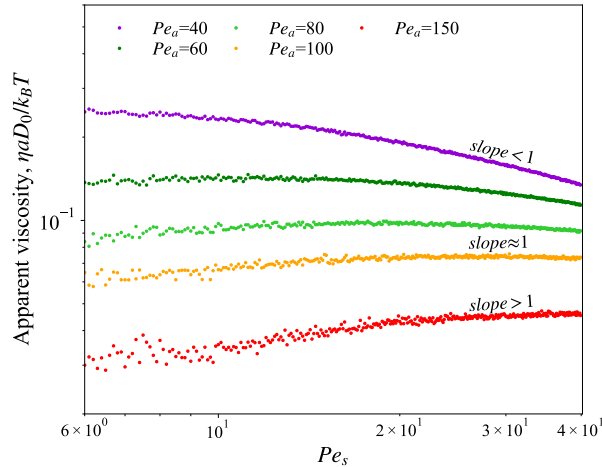


Fig. 3 The apparent viscosity ($\eta = \overline{\sigma}_{xy} / \dot{\gamma}$) with respect to the shear rate $\dot{\gamma}$ at different self-propulsion strengths ($Pe_a \geq 40$).

1.5 The effect of particle density on the stress barrier and the yield stress

We show here the effect of the particle density on the stress barrier during the melting of the passive colloidal suspensions in Fig. 4(a). We obtain a lower stress peak (or barrier) at the initial period of shearing in the dilute suspensions. This proves the tendency of the dilute system for disordering which makes the melting process easier for the suspension. On the other hand, when we compare these two passive systems on the shear stress - shear rate plot [see Fig. 4(b)], they both show a solid-like behaviour, but with different yield stresses. Here, since the dilute system melts more easily than the dense one for the same parameters, its behaviour comes closer to the liquid-like regime.

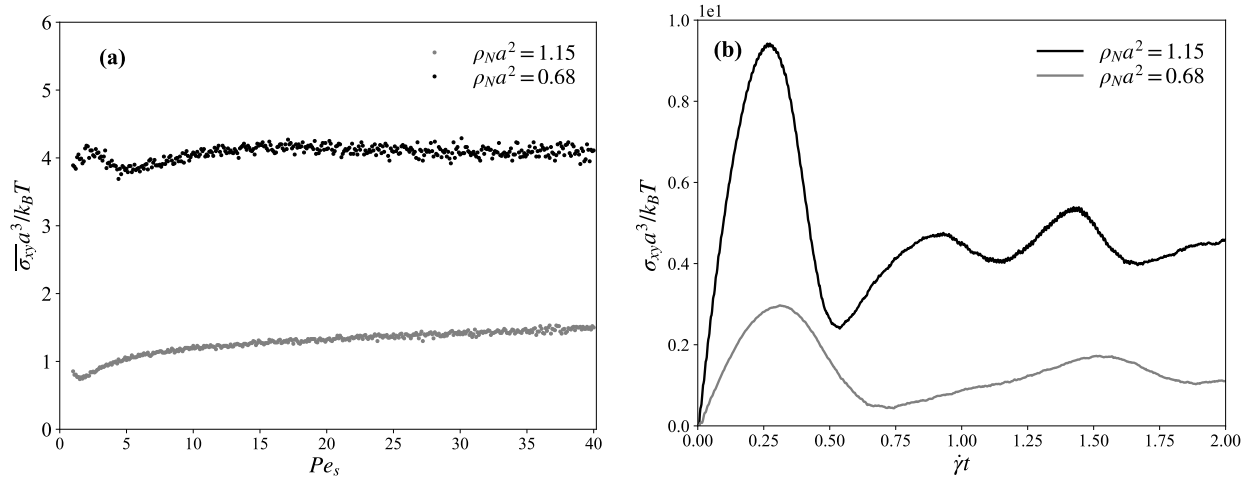


Fig. 4 (a) The nondimensional shear stress $\overline{\sigma_{xy}}$ - shear rate $\dot{\gamma}$ curves for the passive ($Pe_a = 0$) systems and (b) the instantaneous shear stress (σ_{xy}) with respect to strain ($\gamma = \dot{\gamma}t$) at a constant shear rate $Pe_s = 20$ with different particle densities.